Food and Chemical Toxicology 123 (2019) 28–41

Contents lists available at ScienceDirect

Food and Chemical Toxicology

journal homepage: www.elsevier.com/locate/foodchemtox

Metabolism and disposition of arsenic species from oral dosing with sodium arsenite in neonatal CD-1 mice. IV. Toxicokinetics following gavage administration and lactational transfer

Nathan C. Twaddle, Michelle Vanlandingham, Frederick A. Beland, Jeffrey W. Fisher, Daniel R. Doerge*

Division of Biochemical Toxicology, National Center for Toxicological Research, U.S. Food and Drug Administration, Jefferson, AR, 72079, USA

ARTICLE INFO

Keywords:
Arsenic
Toxicokinetics
ICP/MS
Lactation
Neonatal

ABSTRACT

Arsenic is a ubiquitous contaminant, with typical human dietary intake below 1 μg/kg bw/d and extreme drinking water exposures up to ~50 μg/kg bw/d. The formation and binding of trivalent metabolites are central to arsenic toxicity and strong human evidence suggests special concern for early life exposures in the etiology of adult diseases, especially cancer. This study measured the metabolism and disposition of arsenite in neonatal mice to understand the role of maturation in metabolic activation and detoxification of arsenic. Many age-related differences were observed after gavage administration of arsenite, with consistent evidence in blood and tissues for higher exposures to trivalent arsenic species in neonatal mice related to the immaturity of metabolic and/or excretory functions. The evidence for greater tissue binding of arsenic species in young mice is consistent with enhanced susceptibility to toxicity based on metabolic and toxicokinetic differences alone. Lactational transfer from arsenite-dosed dams to suckling mice was minimal, based on no dosing-related changes in the levels of arsenic species in pup blood or milk collected from the dams. Animal models evaluating whole-life exposure to inorganic arsenic must use direct dosing in early neonatal life to predict accurately potential toxicity from early life exposures in children.

1. Introduction

Arsenic is a toxic element distributed ubiquitously throughout the earth's crust (Takami and Frankenberger, 1992), and humans are exposed to arsenic in its inorganic and organic forms through drinking water and food (European Food Safety Authority, 2009). A number of human diseases has been associated with exposure to arsenic, including cancer, cardiovascular disease, and diabetes, and risk assessments by international regulatory bodies have typically used elevated incidences of cancer as critical effects of inorganic arsenic (European Food Safety Authority, 2009; U.S. Environmental Protection Agency, 2010; World Health Organization, 2011; U.S. Food and Drug Administration, 2016). The strongest evidence linking arsenic exposure with diseases comes from heavily exposed populations in the developing world where drinking water contamination can be high (i.e., up to mg/L levels; Mukherjee et al., 2006) with resulting daily intake estimated at up to 50 μg/kg bw. The use of such epidemiological associations, involving large numbers of subjects, often yields statistically significant risks from arsenic exposures even when extrapolated to daily intake levels in developed societies where widespread contamination of water supplies has been largely eliminated and daily intake from food is below 1 μg/kg bw (European Food Safety Authority, 2009; U.S. Environmental Protection Agency, 2010; World Health Organization, 2011; U.S. Food and Drug Administration, 2016). As a result, individual foods that contribute prominently to overall daily intake have been singled out as potential health concerns, especially when children are frequent consumers (e.g., rice-based infant foods and fruit juices).

There is a strong basis for special concern about early life exposures to inorganic arsenic in the etiology of adult diseases (reviewed in Farzan et al., 2013; Thomas, 2013; Tolins et al., 2014; Tsuji et al., 2015; Bommarito and Fry, 2016; Young et al., 2018). The association is especially strong for several cancers, owing to a unique natural experiment that occurred in 1958–1970 in northern Chile where a large community experienced a well-defined switch in its sole source of drinking water, from a lower arsenic-containing river containing 90 μg/L to a highly contaminated one containing 860 μg/L. This switch entailed a change in estimated adult daily intake of arsenic from ~3 μg/kg bw/d to ~30 μg/kg bw/d (estimates based on a 2 L/d water intake

* Corresponding author.
E-mail address: daniel.doerge@fda.hhs.gov (D.R. Doerge).

https://doi.org/10.1016/j.fct.2018.10.046
Received 7 September 2018; Received in revised form 27 September 2018; Accepted 16 October 2018
Available online 17 October 2018
0278-6915/

from all sources for a 70 kg adult; Steinmaus et al., 2014). Now, over 40 years following the switch back to a lower arsenic-containing water source, elevated incidences of several cancers and other diseases have been reported in the cohort born and raised during the period of elevated exposure when compared with a similar group from an adjacent lower exposed region in Chile. Specifically, subjects consuming > 800 μg/L vs. < 110 μg/L starting at birth to 13 years of age had ~3–6-fold greater lung cancer and ~5- to 15-fold greater bladder cancer risk ratios (Steinmaus et al., 2014). Increased incidences of cardiovascular and respiratory diseases associated with early life exposures to arsenic have also been reported for this population (Steinmaus et al., 2016; Roh et al., 2018).

Confirmatory evidence for early life susceptibility to arsenic-induced carcinogenesis comes from animal models (Thomas, 2013). A long-standing discrepancy in cancer research was the inability of adult animal models to recapitulate inorganic arsenic-induced carcinogenesis, as seen in humans (International Agency for Research on Cancer, 2004; International Agency for Research on Cancer, 2012); however, this discrepancy was resolved by the discovery that cancer is produced in multiple organs of mice after either gestational (Waalkes et al., 2003) or "whole-life" exposure to sodium arsenite (Tokar et al., 2011). Animal models for other pathologies associated with early life exposures to inorganic arsenic have been reported, including diabetes (Huang et al., 2018), respiratory disease (Petrick et al., 2009), and fatty liver disease (Ditzel et al., 2016).

The metabolism and disposition of inorganic arsenic and its metabolites appear to be central to the toxicity seen in humans and animal models, as discussed in previous publications (Twaddle et al., 2018a; Twaddle et al., 2018b). While methylation by arsenite methyltransferase (As3MT, Dheeman et al., 2014) appears to facilitate excretion of the ultimate metabolite, DMA^{V}, the formation of reactive trivalent intermediates, MMA^{III} and DMA^{III}, and subsequent binding to critical cellular thiol groups appear key to the toxicity of arsenic (Scheme 1; Shen et al., 2013). Evidence is emerging that metabolic bioactivation by both As3MT (Dheeman et al., 2014; Currier et al., 2016) and enzymatic/non-enzymatic reduction (Delnomdedieu et al., 1994; Styblo et al., 1997; Nemeti and Gregus, 2013; Twaddle et al., 2018a; Twaddle et al., 2018b; Twaddle et al., 2018c) may contribute to toxicity since binding of trivalent species occurred in tissues with both high (e.g., liver) and low (e.g., lung, muscle, brain) levels of As3MT (Kobayashi et al., 2007). Furthermore, the facile exchange of trivalent arsenic between thiol ligands could facilitate transport and binding at sites distal from production (Twaddle et al., 2018a). The dosing level also appears to affect the formation of reactive intermediates since our previous work showed that arsenite doses above 50 μg/kg bw produced non-linear (concave) toxicokinetic responses for bound trivalent arsenic metabolites in adult CD-1 mice, presumably due to metabolic saturation (Twaddle et al., 2018a).

The current study continues our investigation of arsenite metabolism and disposition specifically designed to test the hypothesis that early life susceptibility to inorganic arsenic can stem, in part, from immaturity in metabolic and excretory functions that lead to elevated internal exposures to toxic trivalent species that can disrupt thiol homeostasis (Go and Jones, 2013). And given the unique targets presented during perinatal development (e.g., stem cell differentiation), such elevated exposure to toxic species could irreversibly alter cellular function and tissue development, and affect the susceptibility to diseases later in life. Previously, this work showed that when pregnant CD-1 mice were repeatedly dosed with arsenite in drinking water (1 mg/L), maternal blood and tissues contained "free" DMA^{V} and bound DMA^{III} and MMA^{III}; however, throughout gestation the fetal blood and tissues contained only DMA^{V} and DMA^{III}, which were present at levels similar to those in the dams. The current study extends these findings to include controlled dosing of neonatal CD-1 mice at various ages to understand the relative internal exposures to arsenic metabolites in the post-natal period, including via lactation. The overall goal of these studies is to understand if there is a toxicokinetic/metabolic basis for enhanced tumorigenicity associated with "whole-life" exposure models for inorganic arsenic and its possible utility in assessing risks from early life exposures to arsenic species in the etiology of human diseases, like cancer.

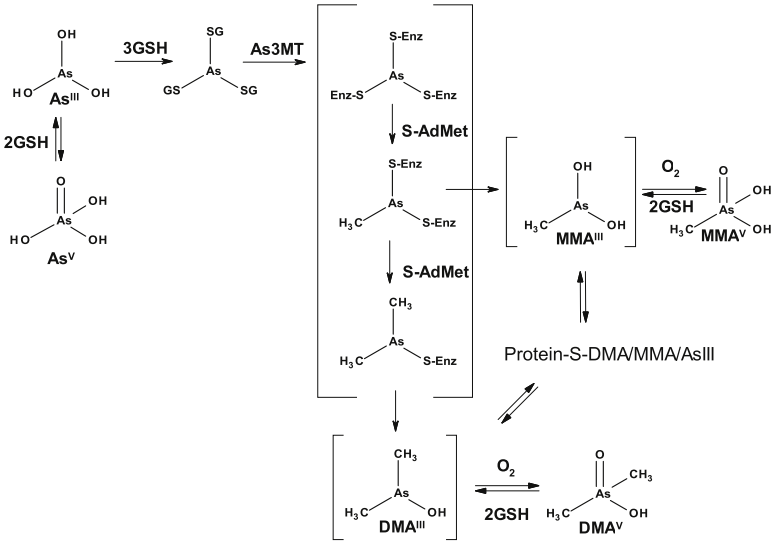

GSH = reduced glutathione
As3MT = arsenite methyltransferase
Enz-S = As3MT catalytic cysteine residues
S-AdMet = S-adenosylmethionine

Scheme 1. Metabolism and binding of arsenite and its metabolites.

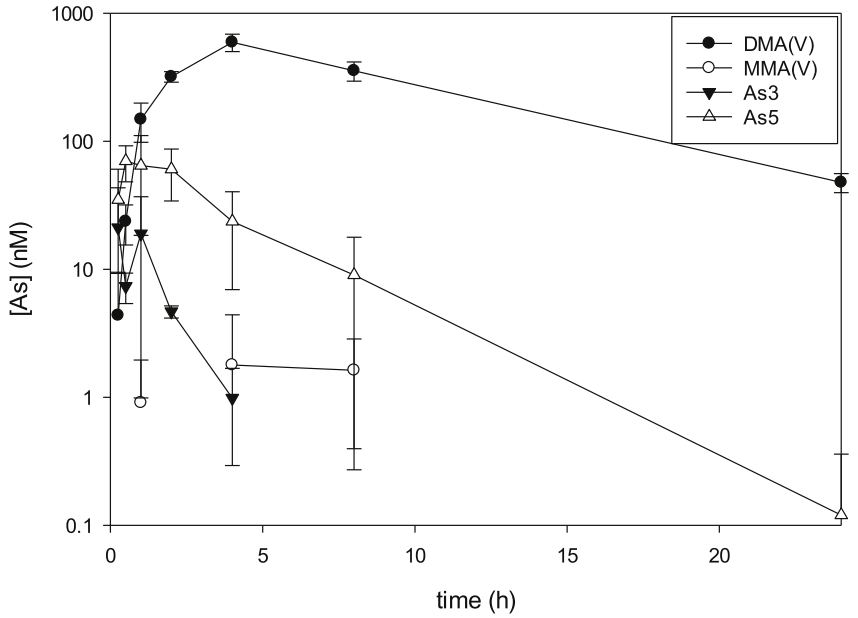

Fig. 1. Plasma time course data for arsenic species in PND 3 neonatal CD-1 mice orally dosed with 50 μg/kg bw sodium arsenite (values plotted represent means of n = 4 pups per time point ± SD).

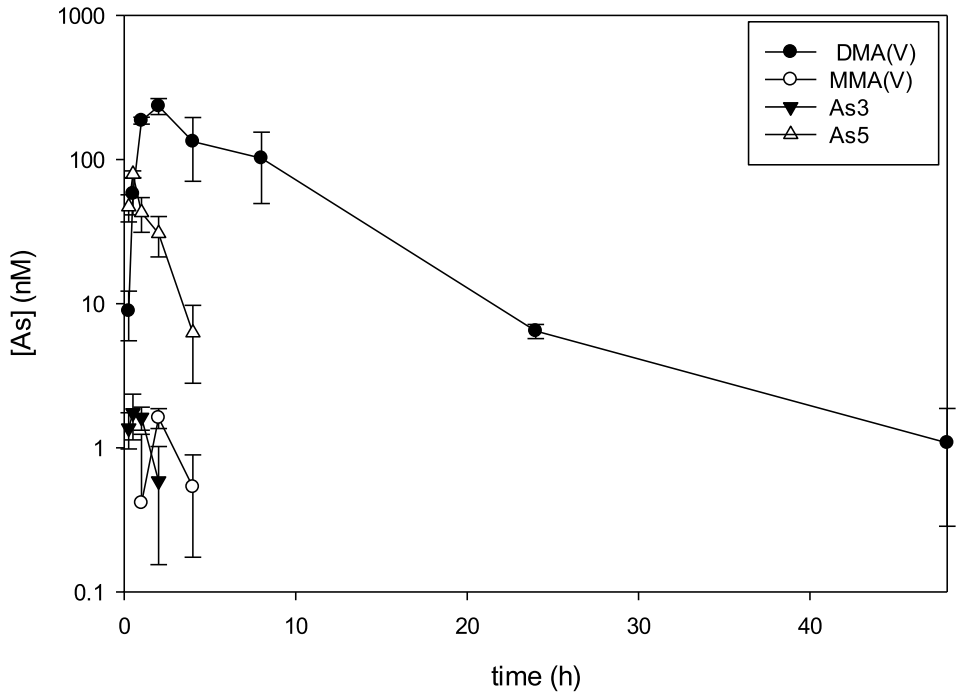

Fig. 2. Plasma time course data for arsenic species in PND 10 neonatal CD-1 mice orally dosed with 50 μg/kg bw sodium arsenite (values plotted represent means of n = 4 pups per time point ± SD).

2. Methods

2.1. Reagents and standards

Hydrogen peroxide (30%) was purchased from Fisher Optima (Thermo Fisher, Waltham, MA); ammonium phosphate dibasic and oxytocin from Sigma-Aldrich (St. Louis, MO); MilliQ-H_2O (18 MΩ) from Millipore (Billerica, MA); and 30 kDa molecular weight cutoff centrifuge filters (30 kD MWCO) from EMD Millipore (Darmstadt, Germany). Blood was collected in EDTA-coated plasma separator tubes (MiniCollect, Greiner Bio-One, Monroe, NC) ranging in size from 0.25 to 1 mL.

NIST-certified solutions (standard reference materials, SRMs) of arsenite and arsenate were purchased from SPEX (Metuchen, NJ). MMA^V (disodium methyl arsenate hexahydrate) and DMA^V (dimethylarsinic acid) were purchased from Chem Service (West Chester, PA), and sodium arsenite was purchased from Lab Chem (Zelienople, PA), and all solutions were prepared by accurately weighing a portion and diluting with MilliQ-H_2O. All dilutions were prepared in opaque polypropylene bottles and stored at 4 °C. All standards were prepared on the basis of elemental As concentration (75 g/mol) and analyzed by infusion into an ICP/MS to ensure an equal As concentration, using arsenate as the reference (NIST SRM 1640A, trace elements in natural water; Gaithersburg, MD).

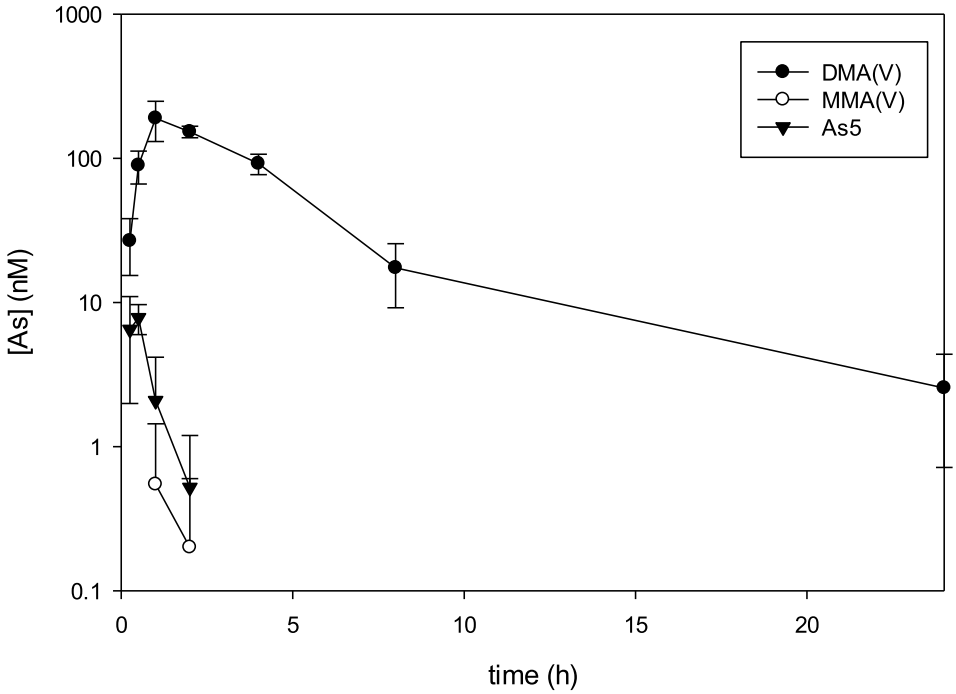

Fig. 3. Plasma time course data for arsenic species in PND 21 neonatal CD-1 mice orally dosed with 50 μg/kg bw sodium arsenite (values plotted represent means of n = 4 pups per time point ± SD).

Table 1
Toxicokinetic parameters for arsenic species in plasma from PND 3, 10, and 21 neonatal CD-1 mice (n = 4 per time point) and adult female CD-1 mice (n = 5–6 per time point) dosed orally with 50 μg/kg bw sodium arsenite (arsenic equivalents). Statistical significance was determined using ANOVA and* indicates a significant difference from the adult group C_{max}, $p < 0.05$.

Group	As Species	$t_{1/2Elim}$ (h)	$t_{1/2Abs\ or\ Form}$ (h)	$AUC_{0-\infty}$ (nM x h)	C_{max} (nM)	T_{max} (h)
PND 3	DMA^V	5.5	2.2	6713	595 ± 93*	4
	MMA^V	–	–	–	1.8 ± 2.6	4
	As^{III}	0.73	0.42	31	21 ± 22*	0.25
	As^V	2.5	0.26	337	70 ± 22*	0.5
PND 10	DMA^V	9.3	0.31	2095	235 ± 30	2
	MMA^V	1.3	0.97	4.2	1.6 ± 0.26	2
	As^{III}	0.68	0.22	3.1	1.7 ± 0.61	0.5
	As^V	1.0	0.16	135	79 ± 4.2*	0.5
PND 21	DMA^V	5.7	0.53	916	190 ± 59	1
	MMA^V	–	–	0.7	0.5 ± 0.9*	1
	As^{III}	–	–	–	–	–
	As^V	0.5	0.07	6.4	7.8 ± 1.8	0.5
Adult	DMA^V	3.9	0.41	892	224 ± 31	1
	MMA^V	2.5	0.44	9.2	2.8 ± 0.6	1
	As^{III}	0.87	0.02	0.9	1.0 ± 0.1	0.5
	As^V	0.60	0.60	4.7	4.6 ± 1.9	0.5

2.2. Liquid chromatography

Ion exchange LC was performed using a Thermo UltiMate 3000 HPLC system (Thermo Scientific, Germering, Germany) consisting of a pump and autosampler. A Hamilton PRP-X100 column (4.1 × 250 mm, 10 μ particle size, Hamilton, Reno, NV), with an isocratic mobile phase consisting of 98% 10 mM ammonium phosphate (pH 8.25, prepared daily) and 2% methanol (Thermo Fisher Scientific) was used for analyte separation/speciation at a flow rate of 1.0 mL/min.

2.3. Mass spectrometry

A Thermo X-Series II ICP-MS (Thermo Electron, Bremen, Germany), equipped with a microflow nebulizer and Peltier-cooled spray chamber maintained at 2 °C (PC3, Elemental Scientific, Omaha, NE), was used to monitor elemental arsenic (*m/z* 75).

2.4. Sample calibration curve

Quantification of each sample set used a series of arsenic standards (arsenite, arsenate, MMA^V, DMA^V) in 10 mM ammonium phosphate (pH 8.25) at defined concentrations to prepare a daily calibration curve. Typically, these standards consisted of a blank along with 3–5 concentrations over a range of 0.05–20 ng/mL As. Linear responses were consistently observed ($R^2 > 0.999$). A typical sample set consisted of calibration standards, a buffer blank, matrix blanks, matrix spikes at multiple concentrations, and incurred samples. Standards were interspersed throughout the sample set to monitor ICP/MS and chromatographic performance. The column effluent was directed through a 10-port switching valve (Rheodyne/IDEX, Lake Forest, IL) that was used to introduce a post-column standard addition of arsenate to provide signal normalization throughout every sample set, as described previously (Twaddle et al., 2018a).

2.5. Method validation

Method validation consisted of spiking plasma or erythrocytes with 3 concentrations of mixed arsenic standards and preparing each concentration in quadruplicate (i.e., 0.1, 1.0, and 10.0 ng/mL) as described previously (Twaddle et al., 2018a). Analysis of mouse milk was validated using commercial half-and-half (100 μL) as a surrogate at arsenic concentrations of 0.1 ng/mL (13 nM) for mixed standards. Accuracy and precision for arsenite, MMA^V, DMA^V, and arsenate were determined from replicate samples (107–126% of nominal with 1.7–33% relative standard deviation). Similarly, tissues were spiked at 5, 10, and 100 ng/g with mixed arsenic standards and homogenized with 10 mg-equivalent aliquots analyzed in quadruplicate on separate days as described previously (Twaddle et al., 2018a).

The method detection limits for arsenic species, which reflect both the presence of low levels of DMA in untreated adult CD-1 mice (Table

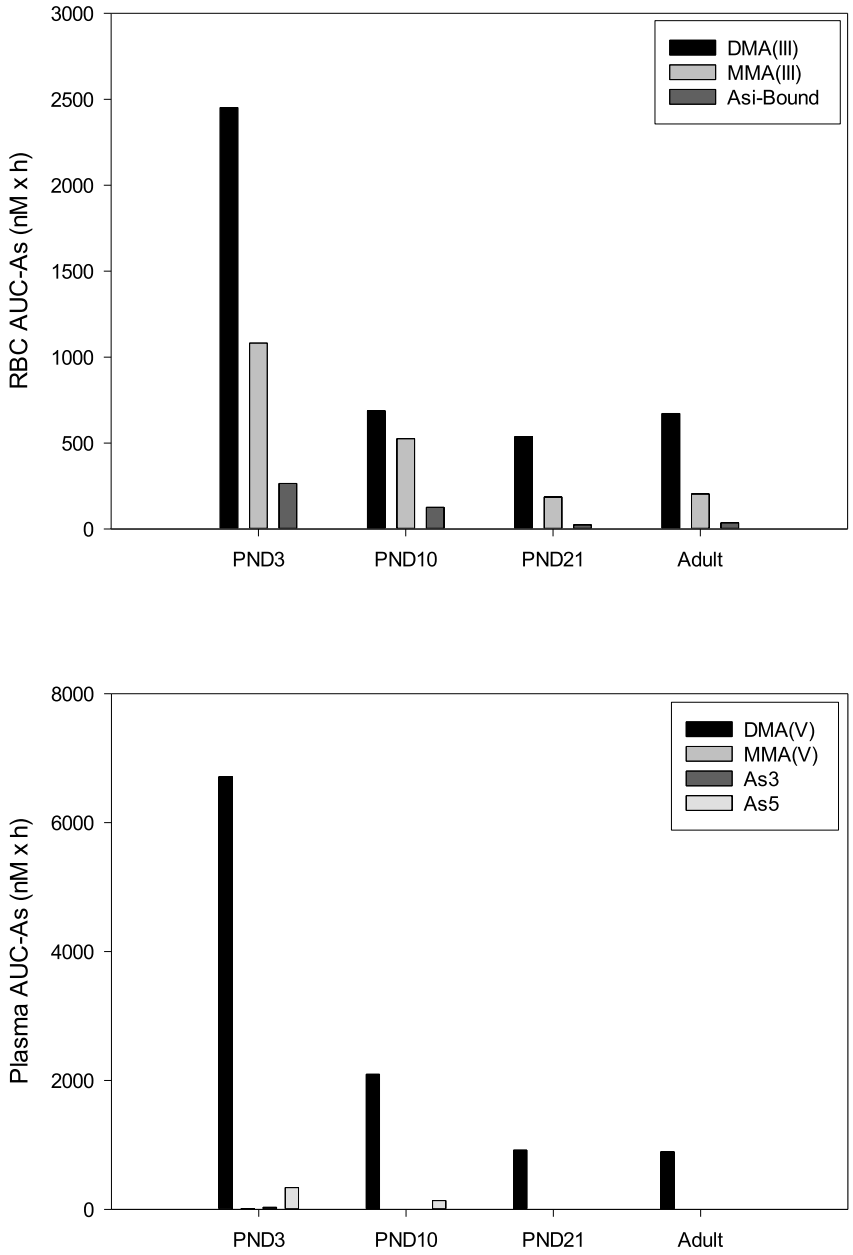

Fig. 4. Comparison of AUCs for different ages of CD-1 mice in plasma ("free" As species, bottom panel) or erythrocytes (thiol-bound As species, top panel).

S1) that were subtracted from dosed samples and sporadic low level contamination by As^V in LC mobile phase and filters, were approximately 1 nM in blood (50 µL) and 1 pmol/g in tissues (10 mg). When arsenic species were detected in mouse milk samples, the remaining extract was fortified with mixed arsenic standards and reinjected to verify the peak assignments and quantification.

2.6. Animal handling procedures

All procedures involving the care and handling of mice were reviewed and approved by the National Center for Toxicological Research Laboratory Animal Care and Use Committee. Charles River Co. (Wilmington, MA) provided pregnant female CD-1 mice and upon arrival, mice were placed on a low-arsenic basal diet (5K96, Test Diets, Purina Mills, Richmond, IN) to reduce the background levels of arsenic present in blood, tissues, and offspring. The analysis of arsenic species in the basal diet were reported previously (Twaddle et al., 2018a). The mean values ± SD from 5 lots of feed were: arsenite (16 ± 0.82 ppb); arsenate (26 ± 3.9 ppb); MMA^V (2 ± 0.2 ppb); DMA^V (17 ± 3.7 ppb); and arsenobetaine (45 ± 12 ppb). Neonatal mice were directly dosed with sodium arsenite by gavage (5 µL/g bw) at 3, 10, and 21 days after birth (post-natal day, PND) when the body weights were 2.6 ± 0.29, 8.5 ± 0.63, and 18.5 ± 1.2 g, respectively (n = 36). Blood was collected by cardiac puncture after CO_2 asphyxiation before dosing (pre-dose) and at various times after dosing, 0.25, 0.5, 1, 2, 4, 8, 24, and 48 h for the preparation of plasma and erythrocyte fractions by centrifugation (n = 2 males and 2 females at each time point). Tissues were collected from mice treated with arsenite by gavage 1 h after dosing because this interval produced maximal tissue levels in previous gavage studies (Twaddle et al., 2018a; Twaddle et al., 2018b; and Twaddle et al., 2018c).

Lactating dams were dosed with arsenite through the drinking water (1 ppm) starting on PND 1 (n = 6 litters) using the procedures previously described (Twaddle et al., 2018b). On PND 10, dams were removed from the litters and administered oxytocin (2 IU in 100 µL of water by intraperitoneal injection) to induce lactation as described by

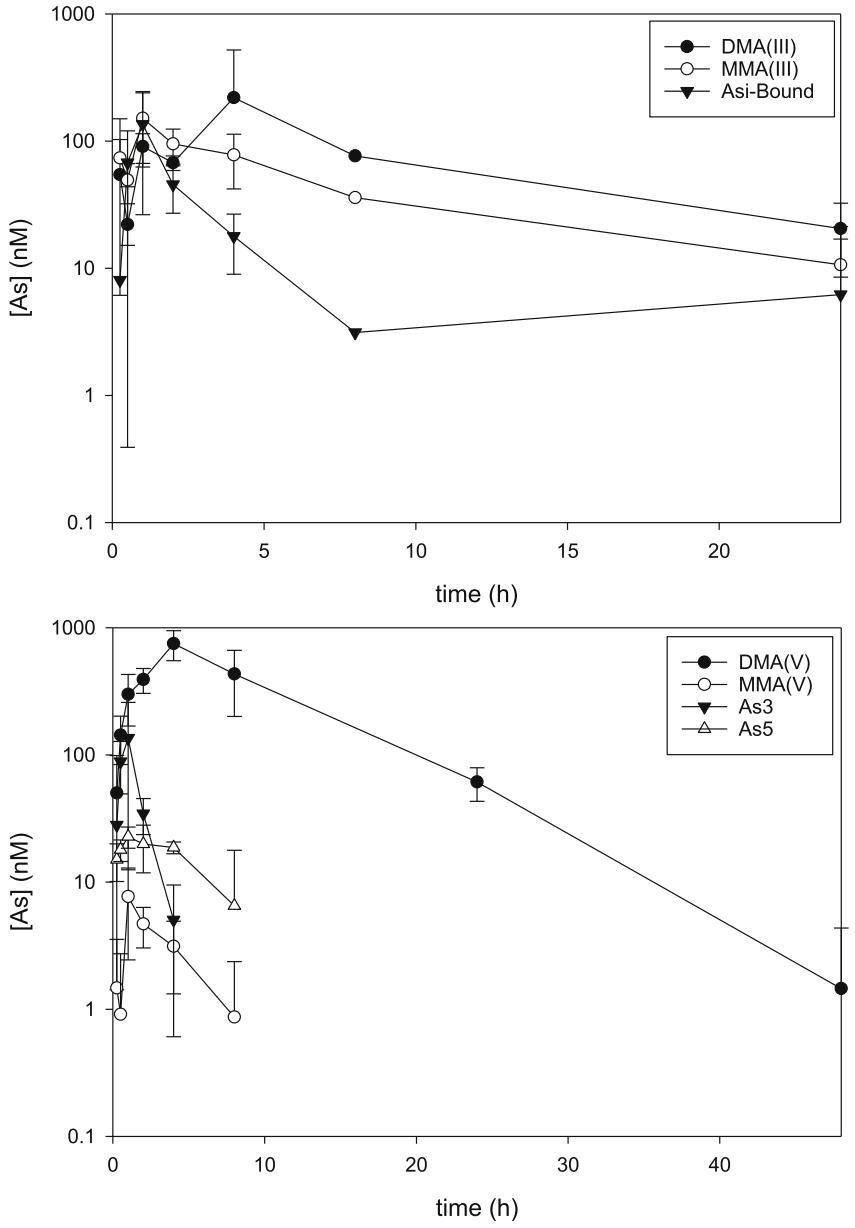

Fig. 5. Time course data for arsenic species in erythrocytes from PND 3 neonatal CD-1 mice orally dosed with 50 μg/kg bw sodium arsenite (values plotted represent means of n = 4 pups per time point ± SD). Thiol-bound trivalent As species are shown in the top panel and "free" species are shown in the bottom panel.

DePeters and Hovey (2009). The dam was then placed in an isolation box within the home cage containing the pups for approximately 10 min. The isolation box was then removed and the dam was allowed to nurse pups for 3–5 min prior to manual milk collection. Milk was collected separately from individual mice and stored frozen at −60 °C until analyzed. Dams and pups were then euthanized and blood was collected for preparation of erythrocytes and plasma. Control dams (n = 5 litters) were treated identically but maintained on As-free drinking water.

Aqueous dosing solutions were prepared by accurately weighing sodium arsenite, diluting with MilliQ H_2O into opaque, polypropylene bottles, and storing in the refrigerator. Stability of gavage dosing solutions was evaluated repeatedly, and no loss of arsenite, or conversion to arsenate, was observed after storage at ambient conditions for 12 months (Twaddle et al., 2018a). Drinking water solutions were prepared using reverse-osmosis H_2O and were evaluated throughout the study to monitor the stability of arsenite and the lack of conversion to arsenate.

2.7. Sample preparation procedures

Plasma, erythrocytes, milk, and tissues were processed as previously described (Twaddle et al., 2018a). Briefly, liquid samples from blood (50–100 μL) and milk (30–50 μL) or tissue homogenates (100 mg) were diluted with ammonium phosphate buffer (pH 8.25) and processed through a 30 kD molecular weight cutoff filter. All samples were analyzed with and without H_2O_2 treatment using LC-ICP/MS to separate and quantify "free" pentavalent arsenic species from determinations before oxidation and to convert bound trivalent species into their pentavalent equivalents through oxidation using H_2O_2. In this way, it was possible to quantify indirectly the bound trivalent arsenic species as the difference between H_2O_2-treated and untreated determinations (Twaddle et al., 2018a). Representative tissue samples were obtained by combining portions taken throughout the respective organs. No special perfusion procedures were used to purge blood from the tissues because no evidence for carryover of arsenic was observed in the time courses and excretion data previously reported (Twaddle et al., 2018a;

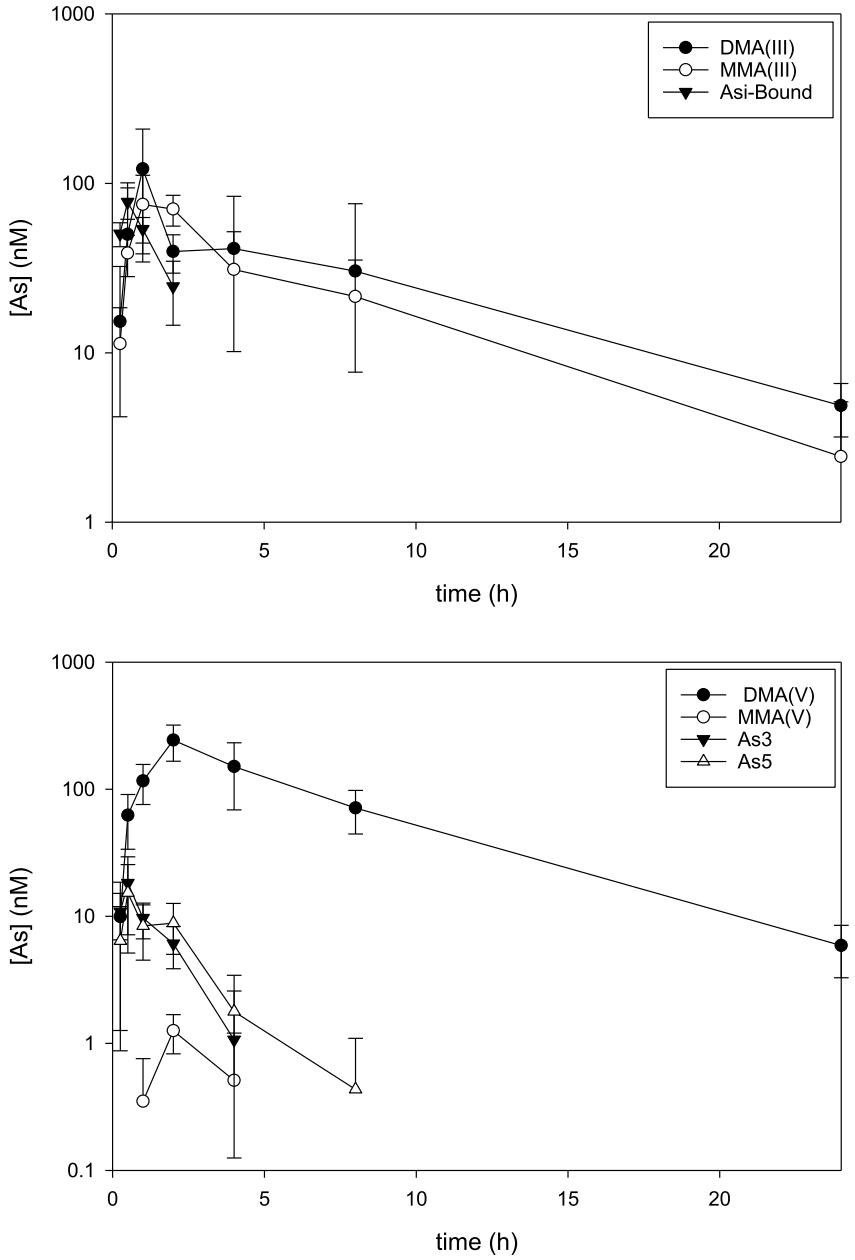

Fig. 6. Time course data for arsenic species in erythrocytes from PND 10 neonatal CD-1 mice orally dosed with 50 μg/kg bw sodium arsenite (values plotted represent means of n = 4 pups per time point ± SD). Thiol-bound trivalent As species are shown in the top panel and "free" As species are shown in the bottom panel.

Gokulan et al., 2018). Tissue and blood samples were stored frozen at −60 °C until analyzed. Repeated analysis of selected blood and tissue samples stored at −60 °C over the course of several months showed no evidence for consistent changes in the determined concentrations of any arsenic species (Twaddle et al., 2018b).

2.8. Toxicokinetic analysis

Plots of average blood (erythrocytes and plasma) concentrations of arsenic species at each time (4 neonatal mice/time point) following bolus gavage administration were analyzed using model-independent (non-compartmental) pharmacokinetic analysis (PK Solutions 2.0 software, Summit Research Services, Montrose, CO). Background levels were determined from buffer blanks and untreated (pre-dose) mouse blood and were subtracted from all time points prior to kinetic analysis. All data points collected were used for the graphical analyses described. Log-linear plots were fit to up to three kinetic phases corresponding to elimination, distribution, and absorption/formation. First-order elimination rate constants (k_{Elim}) were determined from the terminal slope of each curve. First-order distribution and/or absorption rate constants were determined after subtracting the contribution from the terminal elimination phase of the respective curve (i.e., feathering). Half-times were determined from rate constants using the relationship: half-time ($t_{1/2}$) = ln 2/k. Areas under the time-concentration curve ($AUC_{0-\infty}$) for blood measurements were determined by using the trapezoidal rule.

2.9. Statistical analyses

Toxicokinetic parameters were determined from plots of group mean values (n = 4 neonatal mice at each time point). Note that the use of mean values for plasma time points generates composite values for most toxicokinetic parameters that are not amenable to statistical analysis (e.g., half times and AUCs). Values for adult CD-1 mice were from previous studies conducted using identical exposure and analysis

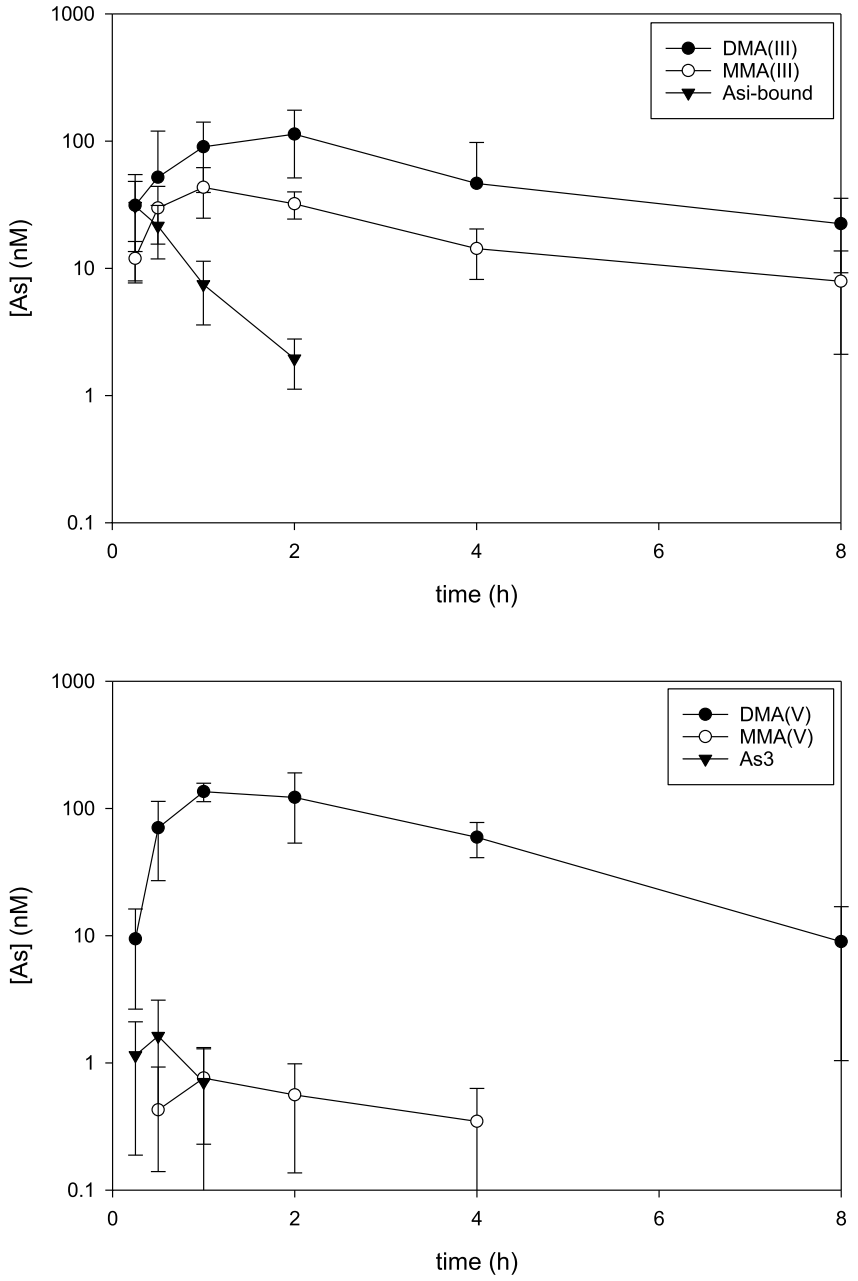

Fig. 7. Time course data for arsenic species in erythrocytes from PND 21 neonatal CD-1 mice orally dosed with 50 μg/kg bw sodium arsenite (values plotted represent means of n = 4 pups per time point ± SD). Thiol-bound trivalent As species are shown in the top panel and "free" As species are shown in the bottom panel.

Table 2
Toxicokinetic parameters for arsenic species in erythrocytes from PND 3 neonatal CD-1 mice dosed orally with 50 μg/kg bw sodium arsenite (arsenic equivalents; n = 4 per time point;* indicates a significant difference from the adult group C_{max}, $p < 0.05$).

As Species	$t_{1/2Elim}$ (h)	$AUC_{0-\infty}$ (nM x h)	C_{max} (nM)	T_{max} (h)
DMA^V	4.9	8703	749 ± 198*	4
MMA^V	2.3	28	7.7 ± 5.2*	1
As^{III}	0.64	203	136 ± 123*	1
As^V	3.9	163	23 ± 4.3*	1
DMA^{III}	22	2452	220 ± 301	4
MMA^{III}	7.1	1082	151 ± 89*	1
As^i-bound	1.6	265	136 ± 110*	1

Table 3
Toxicokinetic parameters for arsenic species in erythrocytes from PND 10 neonatal CD-1 mice dosed orally with 50 μg/kg bw sodium arsenite (arsenic equivalents; n = 4 per time point; (* indicates a significant difference from the adult group C_{max}, $p < 0.05$).

As Species	$t_{1/2Elim}$ (h)	$AUC_{0-\infty}$ (nM x h)	C_{max} (nM)	T_{max} (h)
DMA^V	4.2	1723	243 ± 77*	2
MMA^V	1.5	3.8	1.3 ± 0.43	2
As^{III}	0.89	28	18 ± 11*	0.5
As^V	1.5	34	15 ± 10*	0.5
DMA^{III}	6.9	688	122 ± 87	1
MMA^{III}	5.3	526	75 ± 37	1
As^i-bound	0.90	126	78 ± 16	0.5

Table 4
Toxicokinetic parameters for arsenic species in erythrocytes from PND 21 neonatal CD-1 mice dosed orally with 50 μg/kg bw sodium arsenite (arsenic equivalents; n = 4 per time point).

As Species	$t_{1/2Elim}$ (h)	$AUC_{0-\infty}$ (nM x h)	C_{max} (nM)	T_{max} (h)
DMA^V	1.6	529	135 ± 22	1
MMA^V	2.7	3.3	0.8 ± 0.5	1
As^{III}	0.42	1.5	1.6 ± 1.5	0.5
As^V	–	–	–	–
DMA^{III}	2.7	537	114 ± 62	2
MMA^{III}	2.9	186	43 ± 19	1
As^i-bound	0.44	24	31 ± 17	0.25

conditions (Twaddle et al., 2018c). Where appropriate, group mean values with standard deviations are reported. Neonatal and adult group C_{max} values in blood and tissues were analyzed using one-way ANOVA, using ln transformed data when necessary. Pairwise comparisons were conducted using the Holm-Sidak method. When the ln transformation was unsuccessful, ANOVA on ranks was conducted, with pairwise comparisons being conducted using Dunn's method. Comparisons between dams and their pups were conducted by paired t-tests.

3. Results

3.1. Plasma toxicokinetics

3.1.1. Background exposure

Based on the reported levels of arsenic species in the basal diet reported previously (Twaddle et al., 2018a), liver and brain from untreated neonatal mice (pre-dose) contained detectable levels of DMA^V and DMA^{III} (Table S1). These background levels are similar to those previously reported in the liver and brain from adult female mice (Table S1 and Twaddle et al., 2018c). The respective background values were subtracted from blood and tissue levels determined after dosing with arsenite in order to assess more accurately toxicokinetic parameters that depend on evaluation of terminal elimination (e.g., $t_{1/2Elim}$ and $AUC_{0-\infty}$).

3.1.2. Oral arsenite dosing

Gavage treatment of neonatal mice with 50 μg/kg bw doses of

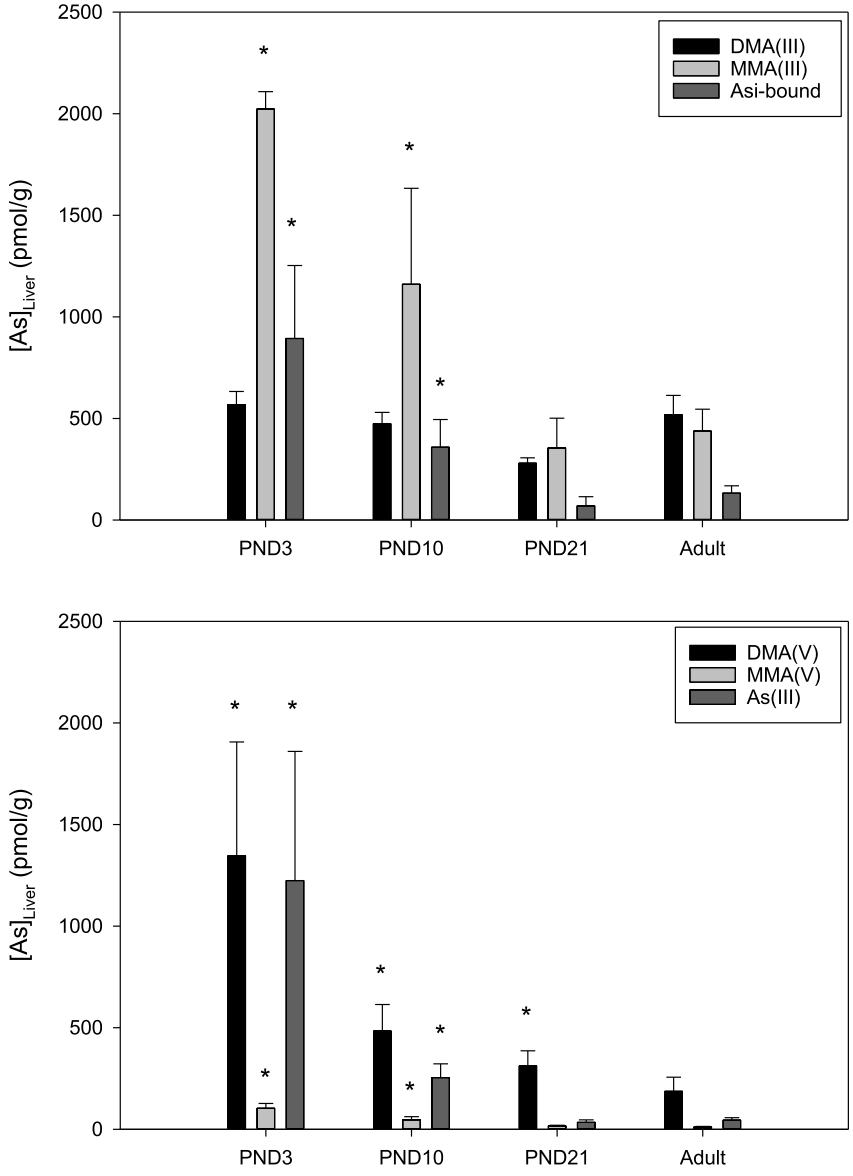

Fig. 8. Concentrations of "free" (bottom panel) and thiol-bound (top panel) arsenic species in liver from different ages of CD-1 mice 1 h after gavage dosing with 50 μg/kg bw sodium arsenite (mean values ± SD; n = 4 pups or 6 adults). Note: * indicates a significant difference from the adult group.

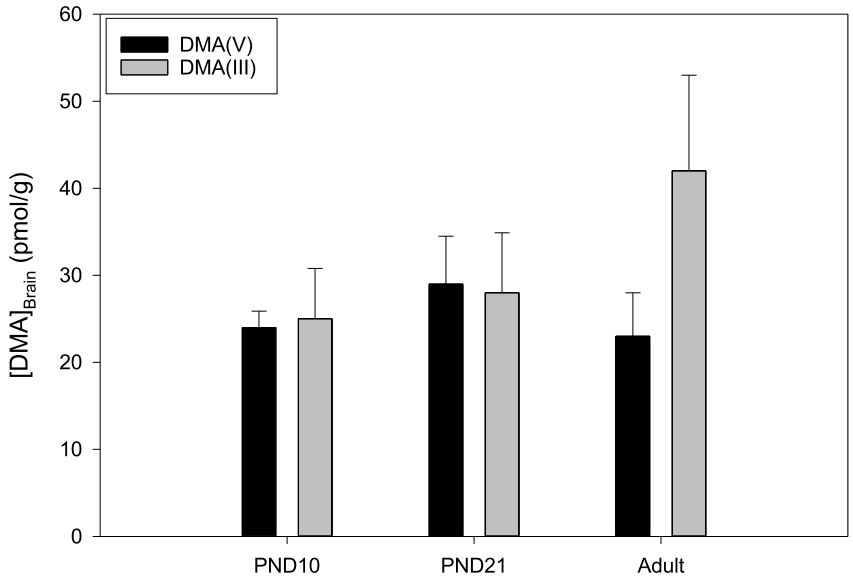

Fig. 9. Concentrations of "free" and thiol-bound arsenic species in brain from different ages of CD-1 mice 1 h after gavage dosing with 50 μg/kg bw sodium arsenite (mean values ± SD; n = 4 pups or 6 adults). Note that measurements were not made for PND 3 brains.

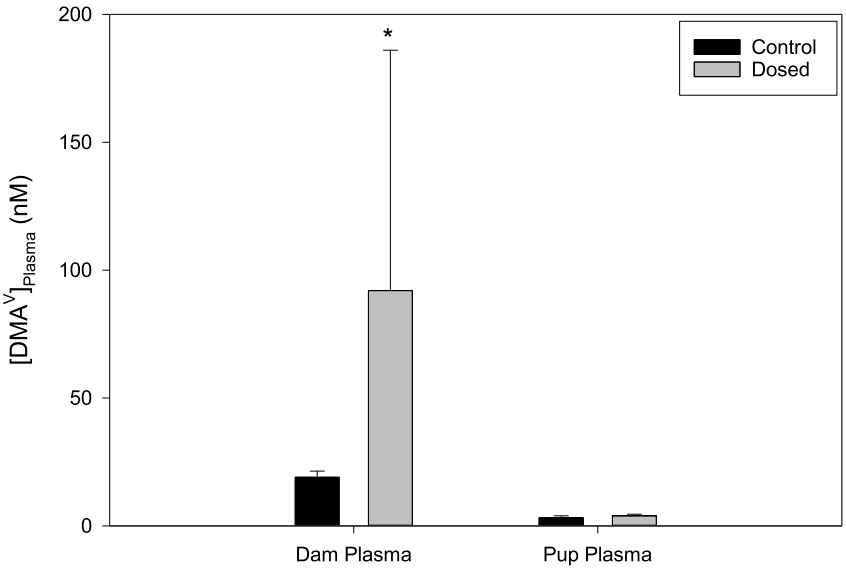

Fig. 10. Concentrations of As species in plasma from control (n = 5 litters) and dosed (n = 6 litters) CD-1 mouse dams and their PND 10 pups (1 ppm sodium arsenite in drinking water). Concentrations of DMA^V in the dosed dams were significantly greater than those in the controls ($p < 0.004$, one-way ANOVA on Ranks) but concentrations of DMA^V in the dosed pups were not different from than those in the controls ($p < 0.079$, one-way ANOVA). Concentrations of DMA^V in the dams were significantly greater than those in their pups ($p < 0.001$ for control and dosed mice using paired t-tests).

sodium arsenite led to rapid appearance of multiple "free" arsenic species in plasma (Figs. 1–3). The short times for appearance of arsenite in plasma indicated rapid absorption (i.e., T_{max} values of 0.25–0.5 h; Figs. 1–3 and Table 1). Comparable values obtained from a previous study in adult female CD-1 mice using identical dosing with arsenite and analysis of blood this (T_{max} = 0.5 h) are also listed in Table 1 (Twaddle et al., 2018c). The rate of absorption appeared to increase with age (i.e., the absorption half-time in PND 3 mice was the largest, Table 1). A corresponding significant effect of age on C_{max} values for arsenite was observed, with the PND 3 value being greater than all other ages. The order for arsenite plasma AUCs was highest in PND 3 group ≫ PND 10 > PND 21 and adult groups (Fig. 4, bottom panel).

The oxidation of arsenite to arsenate was observed in mice of all ages, but the apparent conversion was slowest in PND 3 < PND 10 ≪ PND 21 and adults (Table 1). A significant effect of age on C_{max} values was observed for arsenate, with the values on PND 3 and PND 10 being significantly greater than for adults.

DMA^V was the predominant species observed in plasma for all ages of mice, representing 94–99% of the combined AUCs (Table 1 and Fig. 4, bottom panel). The apparent formation of DMA^V was slowest for PND 3 < PND 10 < PND 21 and adult (Table 1). In mice of all ages, the terminal elimination of DMA^V from plasma was the slowest of the arsenic species measured and the half-times did not appear to change appreciably with age. This combination of kinetic factors led to a significant effect of age on C_{max} for DMA^V, with values in the PND 3 group being greater than all other ages. Limited formation of MMA^V was observed, and was not significantly associated with age.

Analysis of samples with and without H_2O_2 showed that binding of trivalent arsenic species to plasma proteins contributed a small amount to the total arsenic present in plasma (e.g., DMA^{III} was ≤20% of DMA^V, not shown). The plasma AUCs for "free" arsenic species are shown in Fig. 4 (bottom panel). The AUCs for DMA^V and inorganic arsenic species were highest in PND 3 mice, relative to PND 21 and adults, which were similar, and those for PND 10 mice, which were intermediate.

3.1.3. *Erythrocyte toxicokinetics*

Previous studies established the utility of the erythrocyte fraction as an accessible systemic source for measuring both pentavalent "free" species and thiol-bound trivalent arsenic species that can complement the measurements of arsenic species in plasma and tissues (Twaddle

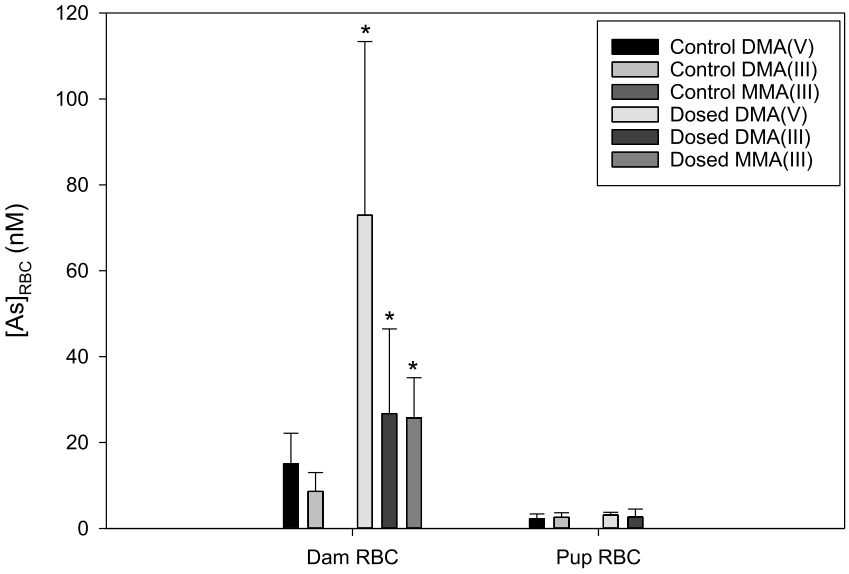

Fig. 11. Concentrations of As species in erythrocytes from control (n = 5 litters) and dosed (n = 6 litters) CD-1 mouse dams and their PND 10 pups (1 ppm sodium arsenite in drinking water). Concentrations of DMA^V ($p < 0.012$), DMA^{III} ($p < 0.029$), and MMA^{III} ($p < 0.004$) in erythrocytes from dosed dams (n = 5 litters) were significantly greater than those from control dams (n = 6 litters) using ANOVA. ANOVA also showed that the DMA^V and DMA^{III} concentrations were not significantly different between control and dosed pups ($p < 0.247$ and 0.940, respectively, using paired t-tests). Concentrations of DMA^V and DMA^{III} in the control dams were significantly greater than those in their pups ($p < 0.012$ and 0.018, respectively, using paired t-tests) and DMA^V, DMA^{III}, and MMA^{III} in the dosed dams were significantly greater than those in their pups ($p < 0.031$, 0.001, and 0.027, respectively).

Table 5
Concentrations of arsenic species in milk collected on PND 7 from control and dosed (1 ppm sodium arsenite in drinking water) CD-1 mouse dams. Note that collection of limited milk volumes required composing samples from control (100 μL) and dosed (124 μL) dams for analysis of each sample with and without addition of H_2O_2. Inorganic As was not observed and detection limits for all species were approximately 1 nM.

Milk	DMA^V (nM)	DMA^{III} (nM)	MMA^V (nM)	MMA^{III} (nM)
Control	30	25	< LOD	< LOD
Dosed	25	5	2	5

et al., 2018a; Twaddle et al., 2018b; Twaddle et al., 2018c). The time courses for "free" DMA^V, MMA^V, and inorganic arsenic species in neonatal mice were generally similar to those observed in the respective plasma (Figs. 5–7). Similar to what was seen in the plasma measurements (see above), there were many significant age-related differences in C_{max} values: all four "free" arsenic species (DMA^V, MMA^V, As^{III}, and As^V) in PND 3 mice were significantly different from adults (Table 2 and Table S2); three of four in PND 10 mice (Table 3 and Table S2); but no differences observed for PND 21 and adults (Table 4 and Table S2). The similar comparison for C_{max} values of thiol-bound trivalent arsenic species in PND 3 mice showed significant age-related differences for MMA^{III} and As^i-bound, with the values decreasing in older mice (Tables 2–4 and Table S2).

There were small apparent age-related differences in elimination half-times for all arsenic species in erythrocytes, with the exception of DMA^{III} in PND 3 mice, where a markedly slower elimination was observed (Tables 2–4 and Table S2). These combinations of kinetic factors led to a large apparent age effect on the AUCs for DMA^V and all bound trivalent species, with PND 3 values being much greater than all other age groups (Figs. 2 and 4).

3.1.4. Tissue measurements

Arsenic species were also measured in neonatal mouse liver and brain, using the 1 h time points for all ages. Similar to the pattern observed in the erythrocytes, there were numerous significant age-related differences between neonatal tissue arsenic concentrations, including both pentavalent and bound trivalent species (Fig. 8): five of six species (MMA^{III}, As^i-bound, DMA^V, MMA^V, and As^{III}) in PND 3 and PND 10 livers were significantly different in PND 21 livers compared to adult values; and one (DMA^V) of six values was different in PND 21 livers. Only DMA^V and DMA^{III} were observed in PND 10, PND 21, and adult brains (Fig. 9), and no effect of age was seen. In addition, the brain levels of DMA^V and DMA^{III} were not significantly different from each other. The brain levels were markedly lower than the corresponding values in liver (Fig. 8).

3.2. Lactational transfer after repeated dosing of dams with sodium arsenite via the drinking water

3.2.1. Plasma measurements

Lactating dams were placed on either control (n = 5 litters) or arsenite-dosed (n = 6 litters) drinking water (1 mg/L) after delivery (PND 1) in order to produce reproducibly elevated levels of arsenic species throughout the body by repeated dosing, albeit dependent on drinking frequency and magnitude. Our previous study of pregnant and non-pregnant CD-1 mice consuming 1 mg/L arsenite in drinking water showed that total daily intake was ~200 μg/kg bw (Twaddle et al., 2018b). On PND 10, blood was collected from the dams and pups for analysis of arsenic species in plasma and erythrocyte fractions. The timing was chosen to ensure that pups had not yet started to consume solid food. DMA^V was the only arsenic species quantified in plasma from both dams and pups (DMA^{III} was present in plasma but not measured (see below for erythrocytes) and all other species were not detected. Arsenic intake from the basal diet produced measurable background levels of DMA^V in plasma from control dams, and, as was observed in our previous drinking water exposure study in adult female CD-1 mice (Twaddle et al., 2018b), a significant increase in plasma DMA^V was observed in the dams consuming arsenite-dosed water (Fig. 10). DMA^V concentrations in plasma from control pups were also measurable and the concentrations were significantly lower than those in their dams. Similarly, DMA^V concentrations in plasma from dosed pups were also measurable and the concentrations were also significantly lower than those in their dams. However, DMA^V concentrations in plasma from dosed litters were not different from those in control litters (Fig. 10).

3.2.2. Erythrocyte measurements

Erythrocytes from control and arsenite-dosed litters were also analyzed (Fig. 11). Erythrocytes from control dams contained measurable DMA^V and DMA^{III}, which were both significantly increased in the dosed dams. In addition, MMA^{III} was observed only in the dosed dams. DMA^V and DMA^{III} were also observed in erythrocytes from control pups but the values were significantly lower than those in their dams. However, neither DMA^V nor DMA^{III} levels in erythrocytes from control pups were

significantly different from that observed in dosed pups. No evidence for MMA was observed in the pups.

3.2.3. Milk measurements

Lactating dams were placed on either control (n = 5 litters) or arsenite-dosed drinking water (1 mg/L, n = 6 litters) on PND 1 through PND 7, at which time milk was collected from the dams for analysis of arsenic species. The small volumes of milk collected from each dam (0–40 μL from control dams and 2–45 μL from dosed dams), the limitations associated with pipetting a viscous liquid, the need to analyze each sample in duplicate (i.e., with and without H_2O_2), and the sample volume requirement for adequate analytical detectability (~50 μL needed for an LOD of 1 nM) made it necessary to pool the respective control and dosed litters into a composite sample for each (Table 5). The milk sample from the control dams contained detectable levels of DMA^V and DMA^{III} and milk from dosed dams contained a similar level of DMA^V and an even lower level of DMA^{III}. In addition, low levels of MMA^V and MMA^{III} were observed in milk from dosed dams. The sampling limitations discussed above precluded statistical testing of the results.

4. Discussion

4.1. Toxicokinetics of sodium arsenite in neonatal CD-1 mice following gavage administration

Bolus oral administration of sodium arsenite to CD-1 mouse pups resulted in plasma toxicokinetics with some superficial similarities to adult mice: rapid and extensive formation of DMA^V, the major metabolite that comprised 94–99% of total arsenic plasma AUC; minimal levels of MMA^V; and similar elimination half-time for DMA^V. However, a general developmental trajectory was evident in plasma, erythrocyte, and liver endpoints, in which internal exposures were highest in PND 3 mice, and reached essentially adult values by PND 21. The notion of such a trajectory was supported by clear age-related differences, including significantly higher C_{max} values (Table 1) and greater AUCs for DMA^V and inorganic arsenic species (Fig. 4, bottom panel). Similarly, analysis of erythrocytes for thiol-bound trivalent arsenic species showed age-related differences, including significantly higher C_{max} values for MMA^{III} and arsenite (Tables 2–4) and higher AUCs for DMA^{III}, MMA^{III}, and arsenite (Fig. 4, top panel). The findings in blood arsenic parameters were supported by the corresponding levels measured in liver, where significantly higher age-related levels of bound (Fig. 8, top panel) and "free" arsenic species (Fig. 8, bottom panel) were found. By contrast, no age-related differences were observed in brain (Fig. 9). A pattern of diminishing tissue exposure is evident in the much higher levels of arsenic species in neonatal and adult livers (Fig. 8) and erythrocytes (Figs. 5–7) compared to brains (Fig. 9). This pattern emphasizes the importance of first-pass metabolism of arsenite after ingestion, first in the intestine and then in the liver, as reported previously in adult mice (Twaddle et al., 2018c). The similar levels of DMA^V and DMA^{III}, and the absence of MMA, in brains from PND 10, PND 21, and adult mice suggest that a barrier to transport and/or metabolic activation exists as early as PND 10.

The significantly increased levels of "free" arsenite (and arsenate) in plasma and bound arsenite in erythrocytes from the youngest mice are consistent with saturation of As3MT enzymatic capacity such that bolus dosing leads to incomplete conversion of the substrate, arsenite as its tri-GSH complex, and/or depletion of the cofactor (S-adenosylmethionine, Scheme 1; Dheeman et al., 2014). In addition, the evidence for significantly elevated fluxes of MMA^{III} in liver and erythrocytes from young mice suggests a greater impact from inorganic arsenic exposures, given the apparent association of MMA^V levels in urine with human diseases (Chung et al., 2009). Finally, the ability of all ages of mice to fully methylate arsenite eventually is apparently minimally affected by age because 94–99% of total plasma AUC is DMA^V. It is therefore likely that age-dependent development of the capacity for renal elimination or other related processes could reduce total clearance of DMA^V from young mice, resulting in the higher observed AUCs.

Since body weight differences alone influence toxicokinetic internal exposure metrics in predictable ways (i.e., allometry), the magnitude of such effects was evaluated (Table S3). The relative body weights for PND 3, 10, 21, and adult mice were approximately 1: 3: 6: 10 g, which when adjusted by body weight to the ¾ power for predicted differences in clearance (U.S. Environmental Protection Agency, 2011), give scaling factors of 1: 0.74: 0.61: 0.55, respectively, for the respective AUCs. These factors reflect the fact that body weight differences predict that larger doses are required in smaller animals to achieve the same internal exposures due to relative blood flows, organ sizes, and metabolic rates only in the absence of specific metabolic differences (e.g., immaturity; Anderson and Holford, 2008). The findings that measured internal exposure metrics for both "free" and bound arsenic species were actually largest in the youngest mice, and decreased with age, emphasize the importance of immaturity of metabolic and/or excretory processes in determining the toxicokinetics of arsenic species. The finding of minimal differences for internal exposures in PND 21 and adult mice (Tables 1 and 4; Figs. 4, 8 and 9) suggests that the metabolic and physiological processes involved in arsenite metabolism and disposition are essentially mature by weaning.

4.2. Lactational transfer of arsenic to neonatal CD-1 mice following dosing of dams with sodium arsenite through drinking water

A critical exposure mode during early neonatal life is lactational transfer of toxicants, and "whole-life" mouse models for arsenite carcinogenicity have assumed, without evidence, that adequate exposure occurred (Tokar et al., 2011). The results presented here vitiate that assumption. Despite evidence for significantly increased exposures to arsenite metabolites, DMA^V, DMA^{III}, and MMA^{III}, in plasma and erythrocytes from dams repeatedly consuming arsenite-dosed drinking water, their pups had very low levels of DMA^V and DMA^{III} (and no MMA species) that were unaffected by the dams repeated consumption of arsenite. Furthermore, a comparison of milk collected from arsenite-dosed and control dams showed evidence of minimal transfer of arsenic species. These findings are consistent with more limited investigations that reported minimal levels of arsenic in milk from dosed rodents (Xi et al., 2010; Markowski et al., 2011; Kozul-Horvath et al., 2012) and findings of minimal arsenic levels in human breast milk collected in high exposure regions (reviewed in Vahter, 2009). The absence of significant lactational transfer has important implications for "whole-life" arsenic cancer models given that exposures during the critical period of perinatal development are predicted to have an increased effect due the metabolic and toxicokinetic factors discussed above.

5. Conclusions

These lines of evidence indicating higher internal exposures of reactive trivalent arsenic species, including DMA^{III}, MMA^{III}, and arsenite, in tissues from young mice suggest that toxicological effects caused by inorganic arsenic exposures would be more pronounced, particularly when coupled with the unique set of targets expressed during early neonatal development. Indeed, this evidence is consistent with increased susceptibility of neonatal mice to inorganic arsenic based on metabolic and toxicokinetic differences alone.

A previous publication examined metabolism and disposition of arsenite in pregnant and fetal CD-1 mice (Twaddle et al., 2018b). That study used repeated dosing with arsenite at a drinking water concentration selected to minimize metabolic saturation and non-linear toxicokinetics (Twaddle et al., 2018a). While maternal levels of DMA^V in plasma and DMA^{III} in erythrocytes and liver were not materially different from those in mouse fetuses throughout gestation, MMA^{III} was found only in maternal blood and tissues. Despite the absence of MMA

in the fetus, the widespread binding of DMA^{III} in fetal tissues was taken as evidence for metabolic activation of arsenite within the fetal compartment concomitant with the likely alteration of protein thiol homeostasis, cellular function, and toxicity (Scheme 1). However, the DMA levels achieved in fetal tissues from the repeated dosing at 200 μg/kg bw/d (< 100 pmol/g) appear to be lower than those of multiple arsenic species resulting from direct dosing of pups at 50 μg/kg bw (as high as 2000 pmol MMA^{III}/g in PND 3 liver).

The toxicokinetic evidence presented in the current study of neonatal mice, where elevated internal exposures to bound DMA^{III}, MMA^{III}, and arsenite all occur, suggests that early neonatal exposures should not be ignored in animal models designed to elucidate chronic arsenic toxicity. Similarly, the accumulated evidence presented here for minimal lactational transfer of reactive arsenic species to pups dictates that direct dosing models (i.e., gavage) are essential to ensure representative internal exposure during early post-natal life.

Finally, the accumulating evidence for significantly elevated human disease risks (e.g., cancer and cardiovascular and respiratory diseases) specifically associated with early life exposure to inorganic arsenic in the Chilean cohort (Steinmaus et al., 2014), coupled with the understanding that whole-life exposure to a ubiquitous contaminant like arsenic is unavoidable, argues that animal models that best reflect this early life susceptibility are needed. These models must adequately integrate any impact from background exposure through the diet and use dosing levels appropriate to the range of human exposures throughout life with an appropriate focus on cancer and non-cancer diseases to describe adequately risks from typical exposures to all appropriate forms of arsenic present in food and water.

Conflicts of interest

The authors declare that there are no conflicts of interest.

Acknowledgements

This study was funded by the National Toxicology Program under an Interagency Agreement between FDA and NIEHS (FDA IAG #224-17-0502 and NIH IAG #AES12013). The authors gratefully acknowledge Dr. Anil Patri, NCTR, for generous access to ICP/MS instrumentation in the NCTR/ORA Nanotechnology Laboratory. The views presented in this article do not necessarily reflect those of the U.S. Food and Drug Administration.

Transparency document

Transparency document related to this article can be found online at https://doi.org/10.1016/j.fct.2018.10.046.

Appendix A. Supplementary data

Supplementary data to this article can be found online at https://doi.org/10.1016/j.fct.2018.10.046.

References

Anderson, B.J., Holford, N.H.G., 2008. Mechanism-based concepts of size and maturity in pharmacokinetics. Annu. Rev. Pharmacol. Toxicol. 48, 303–332.
Bommarito, P.A., Fry, R.C., 2016. Developmental windows of susceptibility to inorganic arsenic: a survey of current toxicologic and epidemiologic data. Toxicol. Res. (Camb.) 5, 1503–1511.
Chung, C.-J., Hseuh, Y.-M., Bai, C.-H., Huang, Y.-K., Huang, Y.-L., Yang, M.-H., Chen, C.-J., 2009. Polymorphisms in arsenic metabolism genes, urinary arsenic methylation profile and cancer. Cancer Causes Control 20, 1653–1661.
Currier, J.M., Douillet, C., Drobna, Z., Styblo, M., 2016. Oxidation state specific analysis of arsenic species in tissues of wild-type and arsenic (+3 oxidation state) methyltransferase-knockout mice. J. Environ. Sci. (China) 49, 104–112.
Delnomdedieu, M., Basti, M.M., Styblo, M., Otvos, J.D., Thomas, D.J., 1994. Complexation of arsenic species in rabbit erythrocytes. Chem. Res. Toxicol. 7, 621–627.
DePeters, E.J., Hovey, R.C., 2009. Methods for collecting milk from mice. J. Mammary Gland Biol. Neoplasia 14, 397–400.
Dheeman, D.S., Packianathan, C., Pillai, J.K., Rosen, B.P., 2014. Pathway of human AS3MT arsenic methylation. Chem. Res. Toxicol. 27, 1979–1989.
Ditzel, E.J., Nguyen, T., Parker, P., Camenisch, T.D., 2016. Effects of arsenite exposure during fetal development on energy metabolism and susceptibility to diet-induced fatty liver disease in male mice. Environ. Health Perspect. 124, 201–209.
European Food Safety Authority, 2009. Scientific opinion of arsenic in food. EFSA J 7, 1351. http://www.efsa.europa.eu/en/efsajournal/pub/1351.
Farzan, S.H., Karagas, M.R., Chen, Y., 2013. In utero and early life arsenic exposure in relation to long-term health and disease. Toxicol. Appl. Pharmacol. 272, 384–390.
Go, Y.-M., Jones, D.P., 2013. Thiol/disulfide redox states in signaling and sensing. Crit. Rev. Biochem. Mol. Biol. 48, 173–181.
Gokulan, K., Arnold, M., Jensen, J., Vanlandingham, M., Twaddle, N.C., Doerge, D.R., Cerniglia, C.E., Khare, S., 2018. Exposure to arsenite in CD-1 mice during juvenile and adult stages: effects on intestinal microbiota and gut-associated immune status. mBio. https://doi.org/10.1128/mBio.01418–18.
Huang, M.C., Douillot, C., Dover, E.N., Stýblo, M., 2018. Prenatal arsenic exposure and dietary folate and methylcobalamin supplementation alter the metabolic phenotype of C57BL/6J mice in a sex-specific manner. Arch. Toxicol. 92, 1925–1937.
International Agency for Research on Cancer, 2004. IARC Monographs on the Evaluation of Carcinogenic Risks to Humans. Vol 84. Some Drinking-water Disinfectants and Contaminants, Including Arsenic. Arsenic in Drinking-water. IARC, Lyon, pp. 39–270.
International Agency for Research on Cancer, 2012. IARC Monographs on the Evaluation of Carcinogenic Risks to Humans. Vol. 100 C. Arsenic, Metals, Fibres, and Dusts. A Review of Human Carcinogens. Arsenic and Arsenic Compounds. IARC, Lyon, pp. 41–93.
Kobayashi, Y., Hayakawa, T., Hirano, S., 2007. Expression and activity of arsenic methyltransferase Cyt19 in rat tissues. Environ. Toxicol. Pharmacol. 23, 115–120.
Kozul-Horvath, C.D., Zandbergen, F., Jackson, B.P., Enelow, R.I., Hamilton, J.W., 2012. Effects of low-dose drinking water arsenic on mouse fetal and postnatal growth and development. PloS One 7, e38249.
Markowski, V.P., Currie, D., Reeve, E.A., Thompson, D., Wise, J.P. Sr, 2011. Tissue-specific and dose-related accumulation of arsenic in mouse offspring following maternal consumption of arsenic-contaminated water. Basic Clin. Pharmacol. Toxicol. 108, 326–332.
Mukherjee, A., Sengupta, M.K., Hossein, M.A., Ahamed, S., Das, B., Nayak, B., Lodh, D., Rahman, M.M., Chakraborti, D., 2006. Arsenic contamination in groundwater: a global perspective with emphasis on the Asian scenario. J. Health Popul. Nutr. 24, 142–163.
Nemeti, B., Gregus, Z., 2013. Reduction of dimethylarsinic acid to the highly toxic dimethylarsinous acid by rats and rat liver cytosol. Chem. Res. Toxicol. 26, 432–443.
Petrick, J.S., Blachere, F.M., Selim, O., Lantz, R.C., 2009. Inorganic arsenic as a developmental toxicant: *in utero* exposure and alterations in the developing rat lung. Mol. Nutr. Food Res. 53, 583–591.
Roh, T., Steinmaus, C., Marshall, G., Ferreccio, C., Liaw, J., Smith, A.H., 2018. Age at exposure to arsenic in water and mortality 30-40 years after exposure cessation. Am. J. Epidemiol. https://doi.org/10.1093/aje/kwy159.
Shen, S., Li, X.-F., Cullen, W.R., Weinfeld, M., Le, X.C., 2013. Arsenic binding to proteins. Chem. Rev. 7769–7792.
Steinmaus, C., Ferreccio, C., Acevedo, J., Yuan, Y., Liaw, J., Durán, V., Cuevas, S., García, J., Meza, R., Valdés, R., Valdés, G., Benítez, H., VanderLinde, V., Villagra, V., Cantor, K.P., Moore, L.E., Perez, S.G., Steinmaus, S., Smith, A.H., 2014. Increased lung and bladder cancer incidences in adults after *in utero* and early-life arsenic exposure. Cancer Epidemiol. Biomark. Prev. 23, 1529–1538.
Steinmaus, C., Ferreccio, C., Acevedo, J., Balmes, J.R., Liaw, J., Troncoso, P., Dauphiné, D.C., Nardone, A., Smith, A.H., 2016. High risks of lung disease associated with early-life and moderate lifetime arsenic exposure in northern Chile. Toxicol. Appl. Pharmacol. 313, 10–15.
Styblo, M., Serves, S.V., Cullen, W.R., Thomas, D.J., 1997. Comparative inhibition of yeast glutathione reductase by arsenicals and arsenothiols. Chem. Res. Toxicol. 10, 27–33.
Takami, S., Frankenberger Jr., W.T., 1992. Environmental biochemistry of arsenic. Rev. Environ. Contam. Toxicol. 124, 79–110.
Thomas, D.J., 2013. The die is cast: arsenic exposure in early life and disease susceptibility. Chem. Res. Toxicol. 26, 1778–1781.
Tokar, E.J., Diwan, B.A., Ward, J.M., Delker, D.A., Waalkes, M.P., 2011. Carcinogenic effects of "whole-life" exposure to inorganic arsenic in CD1 mice. Toxicol. Sci. 119, 73–83.
Tolins, M., Ruchirawat, M., Landrigan, P., 2014. The developmental neurotoxicity of arsenic: cognitive and behavioral consequences of early life exposure. Ann. Global Health 80, 303–314.
Tsuji, J.S., Garry, M.R., Perez, V., Chang, E.T., 2015. Low-level arsenic exposure and developmental neurotoxicity in children: a systematic review and risk assessment. Toxicology 337, 91–107.
Twaddle, N.C., Vanlandingham, M., Churchwell, M.I., Doerge, D.R., 2018a. Metabolism and disposition of arsenic species from controlled dosing with sodium arsenite in adult female CD-1 mice. I. Pilot study to determine dosing, analytical measurements, and sampling strategies. Food Chem. Toxicol. 111, 482–493.
Twaddle, N.C., Vanlandingham, M., Beland, F.A., Doerge, D.R., 2018b. Metabolism and disposition of arsenic species after repeated dosing with sodium arsenite in drinking water. II. Measurements in pregnant and fetal CD-1 mice. Food Chem. Toxicol. 115, 178–184.
Twaddle, N.C., Vanlandingham, M., Fisher, J.W., Doerge, D.R., 2018c. Metabolism and disposition of arsenic species from controlled dosing with sodium arsenite in adult female CD-1 mice. III. Toxicokinetic studies following oral and intravenous

administration. Food Chem. Toxicol. https://doi.org/10.1016/j.fct.2018.09.068. (in press).
U.S. Environmental Protection Agency, 2010. IRIS Toxicological Review of Inorganic Arsenic (Cancer). https://cfpub.epa.gov/ncea/iris_drafts/recordisplay.cfm?deid=219111.
U.S. Environmental Protection Agency, 2011. Recommended use of body weight$^{3/4}$ as a default method in derivation of the oral reference dose. https://www.epa.gov/risk/recommended-use-body-weight-34-default-method-derivation-oral-reference-dose.
U.S. Food and Drug Administration Center for Food Safety and Applied Nutrition, 2016. Arsenic in Rice and Rice Products Risk Assessment Report. . https://www.fda.gov/downloads/Food/FoodScienceResearch/RiskSafetyAssessment/UCM486543.pdf.
Vahter, M., 2009. Effects of arsenic on maternal and fetal health. Annu. Rev. Nutr. 29, 381–399.
Waalkes, M.P., Ward, J.M., Liu, J., Diwan, B.A., 2003. Transplacental carcinogenicity of inorganic arsenic in the drinking water: induction of hepatic, ovarian, pulmonary, and adrenal tumors in mice. Toxicol. Appl. Pharmacol. 186, 7–17.
World Health Organization, 2011. Safety evaluation of certain contaminants in food. Arsenic. WHO Food Additive Series 63, 153–316.
Xi, S., Jin, Y., Lv, X., Sun, G., 2010. Distribution of arsenic by transplacental and early life exposure to inorganic arsenic in offspring rats. Biol. Trace Elem. Res. 134, 84–97.
Young, J.L., Cai, L., States, J.C., 2018. Impact of prenatal arsenic exposure on chronic adult diseases. Syst. Biol. Reprod. Med. https://doi.org/10.1080/19396368.2018.1480076.